

Proceedings of the ASME 2022 International Mechanical Engineering Congress and Exposition IMECE2022 October 30-November 3, 2022, Columbus, Ohio

IMECE2022-97020

Experimental Investigation of Taper Angle and Airflow Rate on Air-injected Bubble Squeezing in a Tapered Microgap

Maharshi Y. Shukla

Department of Mechanical Engineering, Rochester Institute of Technology, Rochester, NY, USA

Satish G. Kandlikar

Department of Mechanical Engineering, Rochester Institute of Technology, Rochester, NY, USA

ABSTRACT

Squeezing bubbles in a tapered microgap has proved to be effective for improving flow stability in flow boiling. A previous study from our research group has successfully demonstrated using tapered microgap for transforming pool boiling into a selfsustained flow boiling-like system for cooling CPU through thermosiphon. To overcome the imaging challenges with nucleating vapor bubbles, the present work investigates the squeezing behaviour of air-injected bubbles between a tapered microgap with taper angles of 5°, 10°, and 15°. The air bubbles are injected at a rate of 3 ml/min, 15ml/min, and 30 ml/min in a pool of water. The bubble squeezing is recorded at 2000fps using a Photron high-speed camera. The experimental analysis compares the displacement and velocity of the advancing and receding bubble interfaces. The analysis found that in certain test cases, multiple bubbles coalesced while exiting the tapered microgap. In all the test cases, the receding interface of the bubble slingshots after detaching pushes the bubble out of the tapered microgap. The result from the current study provides an insight into the bubble flow and squeezing behavior that can be used for optimizing taper microgap geometries to enhance critical heat flux and heat transfer coefficient of two-phase, and air-injected single-phase heat transfer systems.

Keywords: Tapered micro-gap, bubble squeezing, slingshot

NOMENCLATURE

 θ Taper angle, $^{\circ}$ \dot{V} air flowrate, ml/min

V Velocity magnitude of interface, mm/s

1. INTRODUCTION

Boiling is an efficient two-phase heat transfer phenomenon used by researchers for various engineering applications like steam generation in boilers, cooling with two-phase systems, and electronics cooling. Researchers have investigated different means to enhance pool boiling heat transfer like microstructures [1], microchannels [2], enhanced structures [3], and porous coatings [4]. Effects of heater size [5] and liquid height [6] in pool boiling were studied to investigate the impact on critical heat flux (CHF) and heat transfer coefficient (HTC).

Mukherjee and Kandlikar [7,8] analyzed a tapered microchannel configuration to improve flow stability. Kandlikar et al. [9] used open microchannels with a tapered microgap to significant reduction pressure drop compared to a uniform cross-section gap. Balasubramanian et al. [10] dissipated more than 400 W/cm² heat flux using stepped microchannels and reduced pressure drop by 30% by expanding microchannels [11]. Lu and Pan compared 0.5° diverging and parallel microchannels to improve flow stability [12]. Kalani and Kandlikar [13] studied bubble flow patterns over plain and microchannel under tapered microgaps and observed that flow stability was unaffected by rapid bubble growth. They introduced open microchannels with the tapered manifold in flow boiling and obtained high heat fluxes at low-pressure drops. They further found that with a 6° taper, the bubble expansion enables pressure recovery in fluid

flow and thus improves heat transfer, thereby reaching a CHF of 1.07kW/cm² with a pressure drop of just 30 kPa.

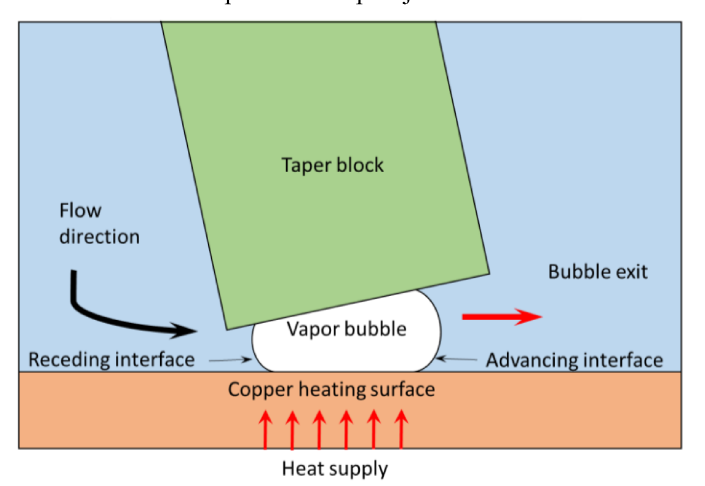


FIGURE 1: BUBBLE SQUEEZING MECHANISM IN TAPERED MICROGAP.

Figure 1 shows the bubble squeezing mechanism between a tapered microgap. As heat is provided to a copper surface, the vapor bubble nucleates and grows in the gap. With a further increase in superheating, the bubble expands and starts to squeeze between the tapered microgap. The surface tension, pressure, and evaporator momentum forces acting on the advancing and receding interfaces push the bubble towards the diverging end of the taper. Chauhan and Kandlikar [14] presented a force balance on the bubble interfaces to calculate the force acting on the bubble for expansion in the expanding direction.

Emery et al. [15] developed a thermosiphon-based CPU cooler using the tapered microgap and HFE 7000 as the working fluid to dissipate a heat flux of over 44 W/cm². Chauhan and Kandlikar [16] further improved the thermosiphon loop performance by testing symmetrical dual taper and dissipating more than 280 W of heat without reaching CHF. Chauhan and Kandlikar [14] proposed using single tapered and symmetrically tapered microgaps in water [17] and HFE 7000 [18] to transform pool boiling into a self-sustained flow boiling mechanism. Tapered microgap has been studied in previous work originating from our research group. Taper angle of 5°, 10°,15°,20°, and 25° with inlet gaps of 0.8 mm and 1.27 mm with HFE 7000 as the working fluid [18]. HTC enhanced by 2x and 1.5x compared to test plain chip without taper when a tapered microgap with a taper angle of 25° was used with an inlet gap of 0.8 mm and 1.27 mm, respectively. The researchers also tested tapered microgap with water at a taper angle of 10° and 15° with an inlet gap of 1.27 mm, and a CHF and HTC enhancement of more than 2x over plain chip was observed [19].

Previously conducted research underlines the difficulty in highspeed visualization of vapor bubble squeezing in tapered microgap under nucleating pool boiling conditions. Therefore, the current work aims to understand the tapered microgap through a bubble-centric approach. In the present work, it is proposed that air-injected bubbles can be used to mimic a nucleating vapor bubble. This approach allows controlling the airflow rate of bubbles and analyzing discrete bubbles without being hampered by the chaotic nucleation of vapor bubbles. The following work aims for a high-speed video analysis of air-injected bubbles squeezing between tapered microgaps of 5°, 10°, and 15° with an airflow rate of 3 ml/min, 15 ml/min, and 30 ml/min. Testing with three different flow rates mimics vapor bubble movement in tapered microgap at different stages of nucleating pool boiling. The result from the present work can be used for finding optimum taper microgap geometry for minimizing the time taken by a bubble to exit the taper.

2. MATERIALS AND METHODS

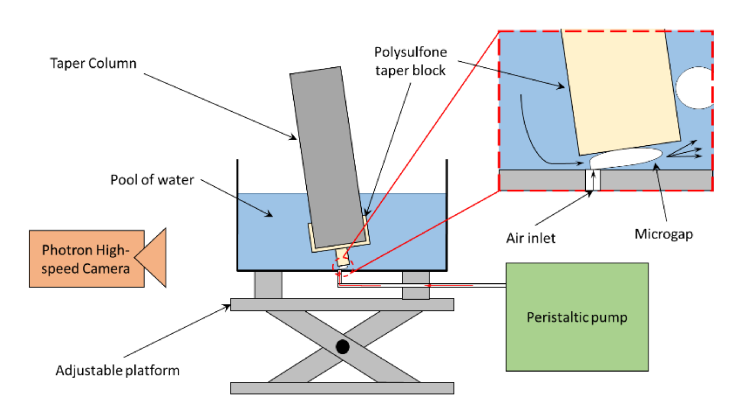


FIGURE 2: SCHEMATIC OF THE EXPERIMENTAL SETUP.

Figure 2 shows a schematic of the setup used in this experimental study. A container with a 1.2 mm orifice is filled with water and placed on an adjustable platform. One end of a flexible tube is connected to the orifice, and the other is connected to a peristaltic pump. The pump can be configured to the desired flow rate for conducting the experiments at different airflow rates. Using an adjustment mechanism coupled at the upper end of the taper column, the polysulfone taper block is immersed in it such that the taper inlet gap is set at 1 mm and the distance from the taper inlet to the center of the orifice is 1.8 mm for any given angle. The walls of the container are fabricated from clear acrylic to enable high-speed imaging. A Photron highspeed camera is set at 2000 fps to capture the squeezing mechanism of the air bubble inside the tapered microgap. The camera is calibrated for pixel size against the known distance of the taper block and against a reference plane to ensure the correct taper angle. Photron Fastcam Viewer (PFV) and Tracker video analysis and modeling tool software are later used to perform the image analysis. Using these software, the advancing and receding interfaces of the bubbles were tracked by marking the

point of the apex of both curvatures. Similar steps of calibration and analysis were performed for all test cases.

3. RESULTS AND DISCUSSION

The following section discusses the analysis of displacement and velocity change in the interface of two scenarios observed from the high-speed videos of bubble squeezing in taper microgap from the experiments performed with 3 ml/min, 15 ml/min, and 30 ml/min airflow rate at taper angles of 5°, 10°, and 15°. In scenario 1, a single bubble squeezes and exits the taper; in scenario 2, two bubbles coalesce and exit the taper. In all the test conditions and scenarios, the air injected bubble always travelled towards the diverging end of the taper, i.e. the taper exit.

3.1 Displacement of receding and advancing interfaces of a bubble in a tapered microgap

The advancing and receding interfaces were tracked from the high-speed videos, and the position of the apex of each curvature with respect to the x-axis was studied. The result from one of the test configurations is plotted in Fig. 3 and Fig. 4.

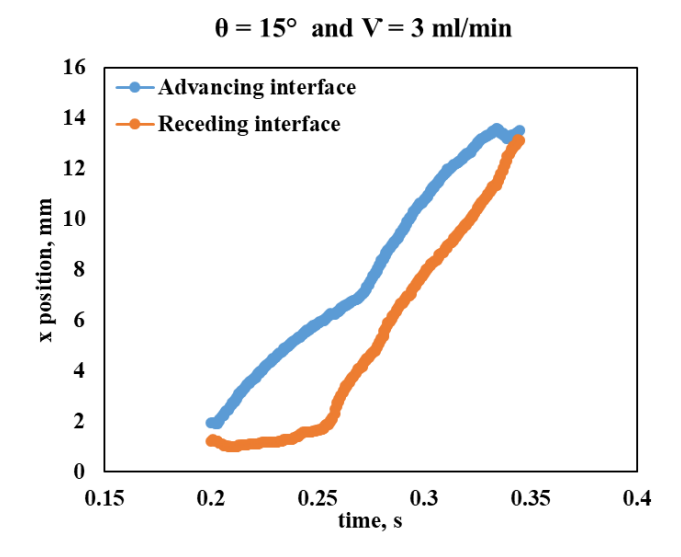


FIGURE 3: DISPLACEMENT OF ADVANCING AND RECEDING INTERFACES OF AIR BUBBLE SQUEEZING BETWEEN A 15° TAPERED MICROGAP WITH AN AIRFLOW RATE OF 3 ML/MIN.

Figure 3 shows the scenario wherein a single bubble is squeezed and exits from the tapered microgap. It illustrates changing the displacement of the x-position of the apex of the advancing and receding interfaces of an air bubble squeezing in a 15° tapered microgap at a flow rate of 3 ml/min. The horizontal axis shows the time taken by the interface of the air bubble to grow and exit the tapered microgap in seconds. The vertical axis shows the x-axis position of the interface apex in mm. The blue marker on the left represents the advancing interface of the air

bubble, and the orange marker on the right represents the receding interface of the bubble. It is observed that initially, as the bubble forms from the orifice, it grows symmetrically until the top surface of the bubble touches the taper surface. Beyond this point, the advancing interface grows in a diverging direction, and the receding interface remains nearly stationary. However, as the bubble ingests more air, the receding interface moves slowly towards the diverging end, reaching the edge of the orifice. The surface tension on the receding interface forces the bubble to detach and move downstream the tapered microgap. The bubble interfaces get squeezed in the tapered microgap and move towards the taper exit with increased acceleration. The force balance inside a bubble being squeezed in a tapered microgap is given by Chauhan and Kandlikar [14]. This action of a sudden increase in bubble velocity as a result of squeezing between tapered microgap is defined as a "slingshot" movement and hereon in the article.

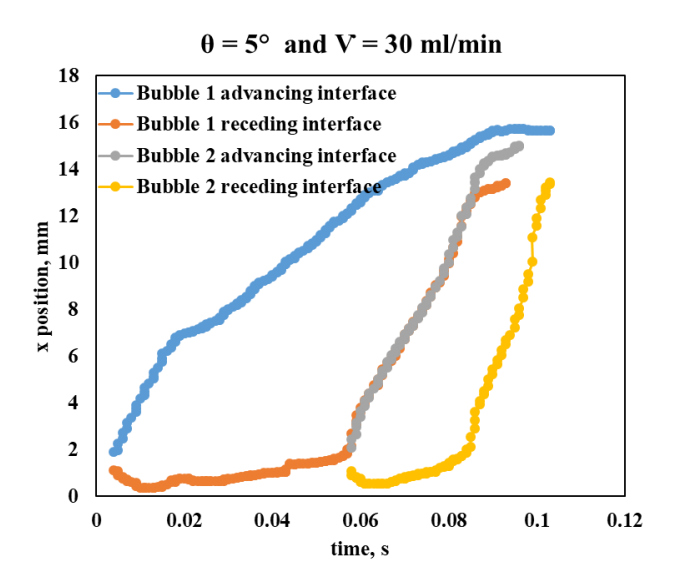


FIGURE 4: CHANGE IN DISPLACEMENT OF ADVANCING AND RECEDING INTERFACES OF TWO AIR BUBBLES SQUEEZING BETWEEN A 5° TAPERED MICROGAP WITH AN AIRFLOW RATE OF 30 ML/MIN.

Figure 4 shows the displacement of advancing, and receding interfaces of air-injected bubbles in scenarios wherein two bubbles coalesce while squeezed in the tapered microgap. The air bubble that appeared first is referred to as the advancing bubble or bubble 1, the bubble that appeared later is referred to as the trailing bubble or bubble 2, and post-fusion, it is referred to as a coalesced bubble. Blue and gray markers show the advancing interfaces, and orange and yellow markers indicate the receding interfaces of leading and trailing bubbles, respectively. The advancing and receding interfaces of the leading bubble behave similarly to the previous case. As the first bubble detaches and moves towards the microgap exit, a new bubble nucleates from the orifice. The advancing interface of the trailing bubble follows the receding interface of the leading

bubble. Both bubbles fuse near the taper exit and form a larger coalesced bubble whose receding interface slingshots towards the taper exit and pushes the bubble off the tapered microgap.

3.2 Velocity of receding and advancing interfaces of a bubble in a tapered microgap

Further high-speed video analysis shows the change in velocity magnitude of the advancing and receding interface. Figure 5 shows the result from the test condition in which the air bubbles were injected at 3 ml/min between 15 tapered microgap. The horizontal axis in Fig. 5 represents the time taken by the bubble to move along the taper in seconds, and the vertical axis shows the velocity magnitude of the interfaces in mm/s. In this scenario, a single bubble nucleated and squeezed between the microgap and the velocity of its advancing interface is shown in blue, and the receding interface velocity is shown in the orange marker. It is observed that initially, the advancing interface grows at a faster velocity than the receding interface, but as the receding interface moves past the orifice, the bubble detaches, and the receding interface slingshots towards the advancing interface. This swift action can be observed by the spike in receding interface velocity around the 0.25-second mark. The slingshotting receding interface thrusts the bubble to the tapered exit with a higher velocity magnitude than before. This movement can be understood further from the high-speed image frames presented later in the paper.

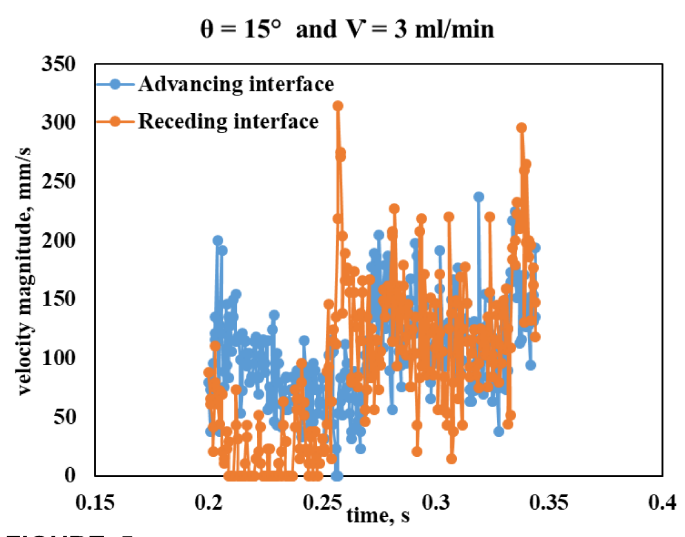


FIGURE 5: CHANGE IN VELOCITY OF ADVANCING AND RECEDING INTERFACE OF AIR BUBBLE SQUEEZING BETWEEN A 15° TAPERED MICROGAP WITH AN AIRFLOW RATE OF 3 ML/MIN.

Figure 6 shows the scenario wherein two bubbles squeeze and coalesces between the taper gap. The vertical axis shows the interface velocity in mm/s, and the horizontal axis represents the time taken by the bubble to grow and leave the taper exit. The marker colors represent the same interfaces as depicted in Fig. 4. It is noted that initially, the advancing interface of the leading

bubble grows at a higher rate, but the velocity drops drastically and then travels towards the taper exit at a velocity of around 200 mm/s. On the other hand, the velocity of the receding interface of leading bubble 1 remains near zero initially, but as the interface slingshots beyond the orifice, it draws a trailing bubble that grows and follows at a similar pace. Towards the taper exit, the receding interface of the leading bubble and advancing interface of the receding bubble fuse with each other and at the same moment, the receding interface of the trailing bubble slingshots towards the taper exit. While the double boost from successive slingshot movements forces the coalesced bubble off the tapered microgap, its velocity is reduced considerably as it exits the taper.

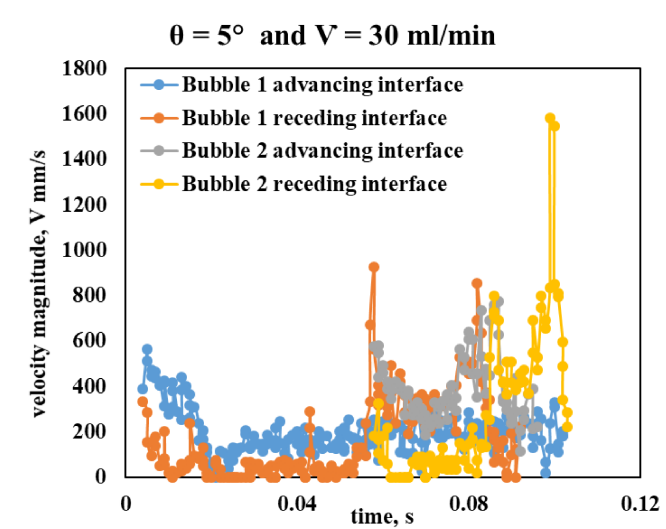


FIGURE 6: CHANGE IN VELOCITY OF ADVANCING AND RECEDING INTERFACE OF AIR BUBBLE SQUEEZING BETWEEN A 5° TAPERED MICROGAP WITH AN AIRFLOW RATE OF 30 ML/MIN.

3.3 Bubble squeezing action through high-speed imaging

To understand air-injected bubbles squeezing in tapered microgap, high-speed videos in Photron Fastcam Viewer. Figure 7 shows six stages of single bubble growth and movement between the microgap for an airflow rate of 3ml/min between a 15° taper. Fig. 8 shows the six stages of two bubbles squeezing and coalescing between tapered microgap wherein the airflow rate is 15 ml/min, and the taper angle is 10°.

Figure 7(a) shows that initially, a bubble develops from the orifice and in roughly 6 ms, the bubble ingests enough air to inflate enough to touch the taper surface. In the next 13 ms, the bubble grows such that the advancing interface moves towards the taper exit, but the receding interface stays still. Further pumping of air squeezes the bubble against the taper surface and forces it to move and grow towards the diverging end of the taper, as seen in Fig 7(d). In roughly another 70 ms, the bubble detaches from the orifice, the receding interface slingshots

towards the advancing interface, and the bubble exits the taper as observed in Fig. 7(e.f).

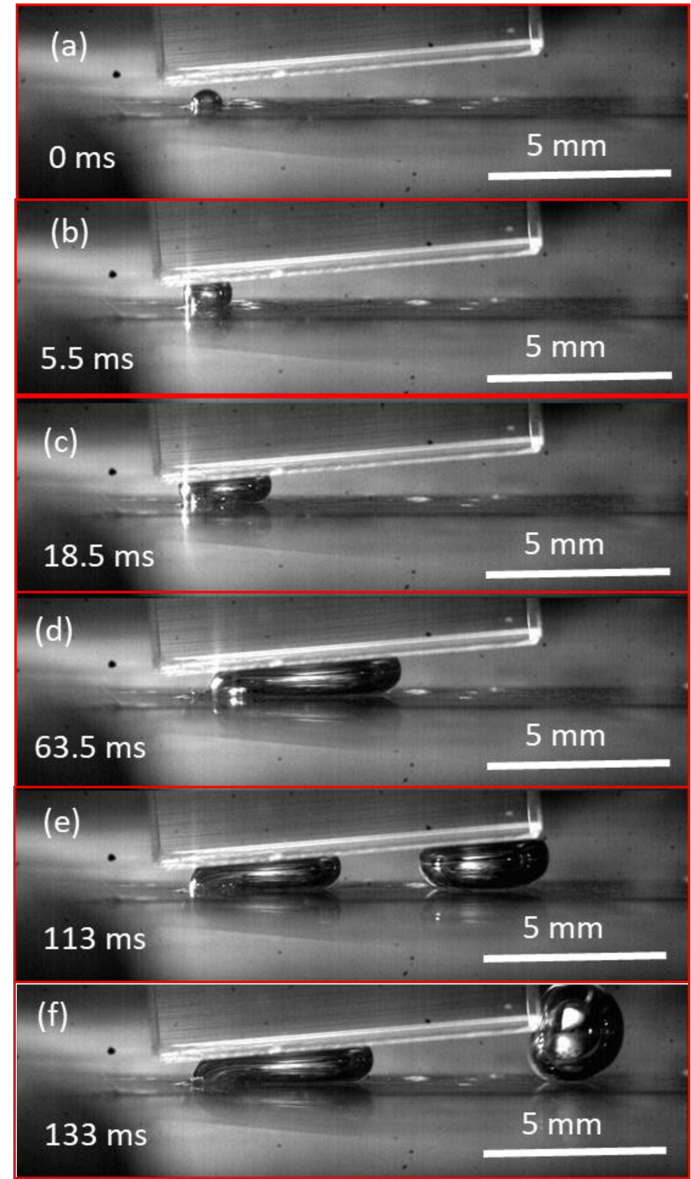


FIGURE 7: HIGH-SPEED VIDEO OF AIR BUBBLE SQUEEZING BETWEEN A 15° TAPERED MICROGAP WITH AN AIRFLOW RATE OF 3 ML/MIN.

Figure 8 shows the case wherein two bubbles squeeze and coalesce together between the tapered microgap. The leading bubble is enclosed in a red dotted line, the trailing bubble is marked with a yellow dotted line, and the coalesced bubble is marked in an orange dotted line.

Initially, a leading bubble grows in the wake of a prior bubble departure. As seen in Fig. 8 (a,b), in approximately 30 ms, the bubble grows in size, squeezes between the tapered microgap, and stretches towards the taper exit. In another 15 ms, the bubble detaches from the orifice and moves in the diverging

direction. As the leading bubble slingshots towards the taper exit, a new bubble nucleates and grows in size, as seen in Fig 8(c,d). The trailing bubble grows rapidly, and just as the leading bubble slows down towards the tapered exit, the trailing bubble slingshots, merges with the leading bubble and forms a large coalesced bubble. Figure 8e shows that in roughly 20 ms, the large coalesced bubble oscillates numerous times before exiting the tapered microgap.

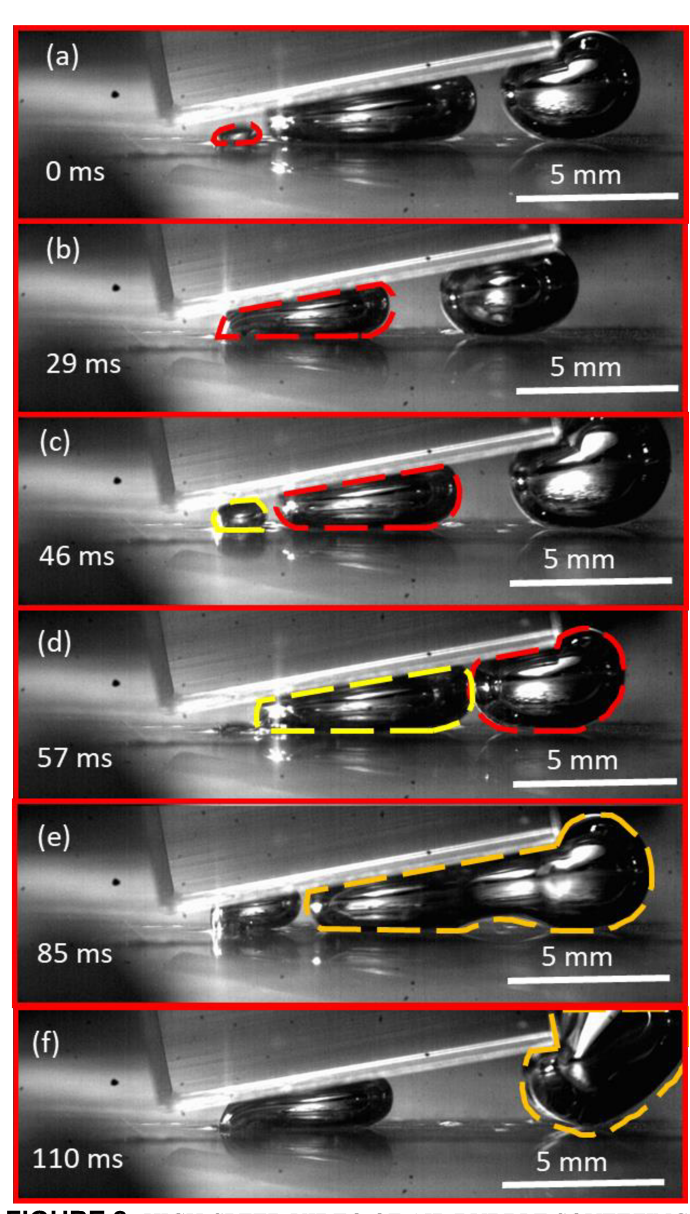


FIGURE 8: HIGH-SPEED VIDEO OF AIR BUBBLE SQUEEZING BETWEEN A 5° TAPERED MICROGAP WITH AN AIRFLOW RATE OF 30 ML/MIN. THE LEADING BUBBLE IS MARKED IN RED MARKER, THE TRAILING BUBBLE IS MARKED IN YELLOW, AND THE COALESCED BUBBLE IS MARKED IN ORANGE DASHES.

The result from different experimental tests can be classified into two scenarios discussed earlier. While most configurations showed just one type of behaviour, specific configurations exhibited both scenarios. The time taken in seconds by air injected squeezing bubble(s) in each configuration between tapered microgap is listed in Fig. 9. The time taken by air inject bubble to exit taper will help understand the behavior of nucleating bubbles under boiling conditions.

Time period for bubble exit from taper microgap

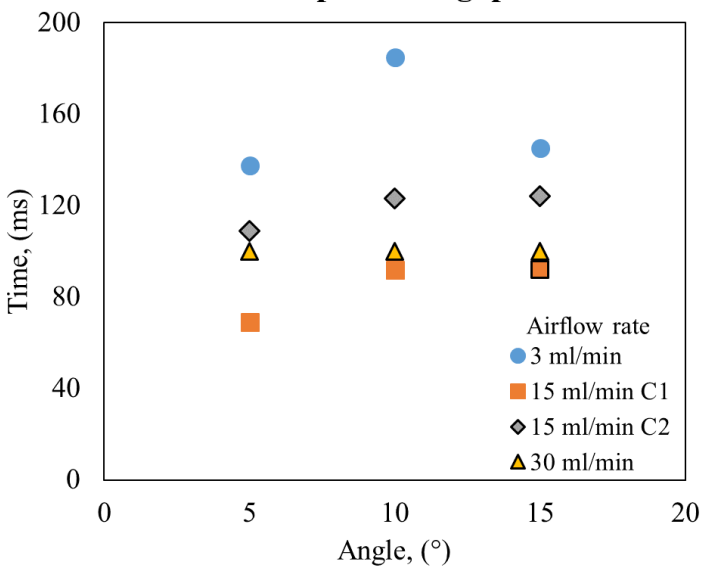


FIGURE 9: TIME TAKEN FOR AN AIR BUBBLE MOVING IN A TAPER MICROGAP AT DIFFERENT AIRFLOW RATES. THE MARKERS WITH BLACK OUTER BORDER SHOW SCENARIOS WHEREIN MULTIPLE BUBBLES COALESCED BEFORE EXITING THE TAPERED MICROGAP.

4. CONCLUSION

The present work studies the impact of air bubble squeezing between a tapered microgap in a pool of water. The current work injects air through a peristaltic pump to mimic a nucleating bubble. Bubble squeezing in tapered microgap with 5°, 10°, and 15° taper angles was studied with an airflow of 3 ml/min, 15 ml/min, and 30 ml/min. It was observed that under all scenarios, the air injected bubble grows, detaches, and moves towards the diverging end of the taper microgap. It was noticed that while the leading interface continues to move at a near-constant rate, the receding interface initially remains constant but then slingshots towards the taper exit to push the bubble forward. Under some scenarios, the leading bubble slows down such that the subsequent bubble coalesces and forms an oscillating slug. The current work allows understanding the behavior of a bubble in a tapered microgap and enables further optimization of the tapered geometry for increasing fluid flow through the gap.

5. ACKNOWLEDGEMENT

The authors gratefully acknowledge the support from National Science Foundation under an NSF- CBET grant.

REFERENCES

- [1] Ahn, H. S., Jo, H. J., Kang, S. H., and Kim, M. H., 2011, "Effect of Liquid Spreading Due to Nano/Microstructures on the Critical Heat Flux during Pool Boiling," Appl. Phys. Lett., **98**(7), p. 071908.
- [2] Cooke, D., and Kandlikar, S. G., 2012, "Effect of Open Microchannel Geometry on Pool Boiling Enhancement," International Journal of Heat and Mass Transfer, 55(4), pp. 1004–1013.
- [3] Hayes, A., Raghupathi, P. A., Emery, T. S., and Kandlikar, S. G., 2019, "Regulating Flow of Vapor to Enhance Pool Boiling," Applied Thermal Engineering, 149, pp. 1044–1051.
- [4] Seo, H., Chu, J. H., Kwon, S.-Y., and Bang, I. C., 2015, "Pool Boiling CHF of Reduced Graphene Oxide, Graphene, and SiC-Coated Surfaces under Highly Wettable FC-72," International Journal of Heat and Mass Transfer, **82**, pp. 490–502.
- [5] Mody, F., Chauhan, A., Shukla, M., and Kandlikar, S. G., 2022, "Evaluation of Heater Size and External Enhancement Techniques in Pool Boiling Heat Transfer with Dielectric Fluids," International Journal of Heat and Mass Transfer, 183, p. 122176.
- [6] Shukla, M. Y., and Kandlikar, S. G., 2021, "Influence of Liquid Height on Bubble Coalescence, Vapor Venting, Liquid Return, and Heat Transfer in Pool Boiling," International Journal of Heat and Mass Transfer, 173, p. 121261.
- [7] Mukherjee, A., and Kandlikar, S. G., 2008, "Numerical Study of the Effect of Inlet Constriction on Bubble Growth During Flow Boiling in Microchannels," American Society of Mechanical Engineers Digital Collection, pp. 73–80.
- [8] Mukherjee, A., and Kandlikar, S. G., 2009, "The Effect of Inlet Constriction on Bubble Growth during Flow Boiling in Microchannels," International Journal of Heat and Mass Transfer, **52**(21), pp. 5204–5212.
- [9] Kandlikar, S. G., Widger, T., Kalani, A., and Mejia, V., 2013, "Enhanced Flow Boiling Over Open Microchannels With Uniform and Tapered Gap Manifolds," Journal of Heat Transfer, 135(6).
- [10] Balasubramanian, K., Lee, P. S., Teo, C. J., and Chou, S. K., 2013, "Flow Boiling Heat Transfer and Pressure Drop in Stepped Fin Microchannels," International Journal of Heat and Mass Transfer, 67, pp. 234–252.
- [11] Balasubramanian, K., Lee, P. S., Jin, L. W., Chou, S. K., Teo, C. J., and Gao, S., 2011, "Experimental Investigations of Flow Boiling Heat Transfer and Pressure Drop in Straight and Expanding Microchannels

- A Comparative Study," International Journal of Thermal Sciences, **50**(12), pp. 2413–2421.
- [12] Lu, C. T., and Pan, C., 2008, "Stabilization of Flow Boiling in Microchannel Heat Sinks with a Diverging Cross-Section Design," J. Micromech. Microeng., **18**(7), p. 075035.
- [13] Kalani, A., and Kandlikar, S. G., 2015, "Flow Patterns and Heat Transfer Mechanisms during Flow Boiling over Open Microchannels in Tapered Manifold (OMM)," International Journal of Heat and Mass Transfer, 89, pp. 494–504.
- [14] Chauhan, A., and Kandlikar, S. G., 2020, "Transforming Pool Boiling into Self-Sustained Flow Boiling through Bubble Squeezing Mechanism in Tapered Microgaps," Appl. Phys. Lett., 116(8), p. 081601.
- [15] Emery, T. S., Del Plato, E., Kandlikar, S. G., and Chauhan, A., 2017, "CPU Cooling with a Thermosiphon Loop with Tapered Manifold (OMM)," 2017 16th IEEE Intersociety Conference on Thermal and Thermomechanical Phenomena in Electronic Systems (ITherm), pp. 864–870.
- [16] Chauhan, A., and Kandlikar, S. G., 2019, "Characterization of a Dual Taper Thermosiphon Loop for CPU Cooling in Data Centers," Applied Thermal Engineering, 146, pp. 450–458.
- [17] Chauhan, A., and Kandlikar, S. G., 2019, "High Heat Flux Dissipation Using Symmetric Dual-Taper Manifold in Pool Boiling," *ICNMM2019*, ASME 2019 17th International Conference on Nanochannels, Microchannels, and Minichannels.
- [18] Chauhan, A., and Kandlikar, S. G., 2022, "Geometrical Effects on Heat Transfer Mechanisms during Pool Boiling in Dual Tapered Microgap with HFE7000," International Journal of Heat and Mass Transfer, 183, p. 122165.
- [19] Chauhan, A., and Kandlikar, S. G., 2020, "High Speed Imaging of Bubble Interface Motion in a Tapered Microgap," American Society of Mechanical Engineers Digital Collection.